

Glacial lake outburst flood at Kedarnath, Indian Himalaya: a study using digital elevation models and satellite images

Sayantana Das · Nabendu Sekhar Kar · Sunando Bandyopadhyay

Received: 29 July 2014 / Accepted: 17 January 2015 / Published online: 29 January 2015
© Springer Science+Business Media Dordrecht 2015

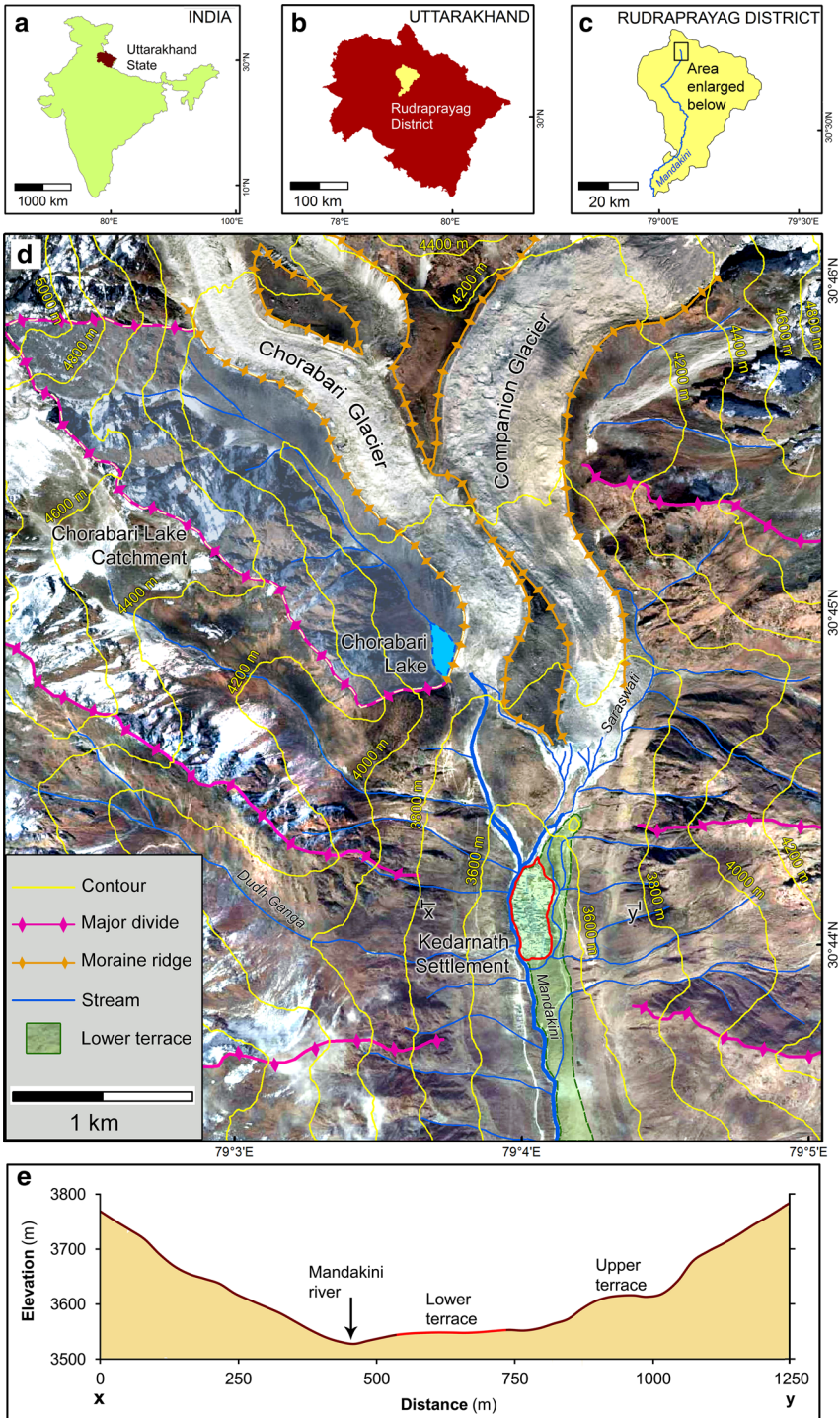
Abstract Kedarnath (3,533 m, 30°44′05″N, 79°04′02″E) is situated within a kilometre of the termini of the Chorabari and Companion glaciers in the Indian Himalaya. An outburst flood from a lake (3,845 m) formed by right lateral moraine of the former caused severe damage to the village on 17 June 2013. We determined various physical parameters of the lake from three digital elevation datasets (CartoDEM, SRTM and ASTER) and selected the SRTM-derived data as they appeared to portray the region more accurately. The obtained parameters were used in predictive equations suggested by different authors to estimate peak discharge of the flood. We also compared high-resolution images of 10 December 1965 (Corona), June 2011 (Bing) and 25 June 2013 (Catrosat-1 Pan + LISS-4mx) to assess the damage caused to the village besides other geomorphic changes. The results showed that at least 149 mm of rainfall in its 291-ha catchment was required to fill up the lake, without considering the presence of antecedent water and loss from seepage and evaporation. At the point of breaching, the lake released $0.43 \times 10^6 \text{ m}^3$ of water with a peak discharge of 1,352 cumecs. The north-western section of Kedarnath village was on the direct path of the debris flow triggered by the flood and was almost completely destroyed. The southern and south-eastern sections were least affected. Out of 37,299 m^2 of pre-event roof area of Kedarnath (259 structures), 44.2 % were obliterated and 26.7 % were partly damaged, representing 138 and 56 structures, respectively. Only one-quarter of the structures of the village emerged intact or slightly affected after the event.

Keywords GLOF · DEM · Remote sensing · Chorabari · Kedarnath

1 Introduction

Bursting of glacial lakes and consequent flooding, widely known as glacial lake outburst flood (GLOF), is a major hazard of the high-altitude river valleys. GLOF is an umbrella

S. Das · N. S. Kar · S. Bandyopadhyay (✉)
Department of Geography, University of Calcutta, 35 Ballygunj Circular Road, Kolkata 700019, India
e-mail: sunando@live.com



◀ **Fig. 1** Location and physiographic setting of the Chorabari lake, its catchment and Kedarnath village at the vicinity of the Chorabari and Companion glaciers. Contours, lake catchment and other topographical elements are extracted from SRTM data of 2000 and superposed on November 2011 image of Bing Maps. Red colouration in topographical profile of **e** shows the extent of Kedarnath settlement on the lower terrace

term that embraces many types of events leading to rapid discharge of glacial lakes. The triggering mechanism of GLOF can range from glacial calving and mass movements into the lake to high-intensity rainfall and snowmelt that lead to the failure of the barrier holding the lake water and downstream propagation of an outburst flood wave (Iturrizaga 2011; Worni et al. 2013; Westoby et al. 2014a). This may emulate a ‘clear water’ flow of low viscosity or, more commonly, debris flow with materials derived from the breached barrier and entrained during run-out (Westoby et al. 2014a).

Remote sensing can help in GLOF studies in three ways. Firstly, it can be used to identify potentially dangerous lakes with possibilities of outburst. Secondly, it can aid to assess volumes of lake depressions and pathways of floodwater from optical stereo image- or synthetic aperture radar (SAR)-based digital elevation models (DEMs). Finally, analyses of pre- and post-flood images can be undertaken for the appraisal of damage and geomorphic change. Using remote sensing sources, Govindha Raj and Kumar (2013) estimated that the Uttarakhand state of Indian Himalaya contains 362 glacial lakes of various types, of which 18 are formed by blocking of valley-side drainage by deposits like avalanche cones and lateral moraines. Worni et al. (2013) estimated that 14 >1 ha lakes of the state are potentially critical for GLOF. Most glaciers of this part of the Himalaya are retreating for the last 200–300 years as the Little Ice Age (LIA) ended (Sharma and Owen 1996). This trend, increasingly operational during the last few decades, indicates a warming environment conducive for the proliferation of glacial lakes and occurrence of GLOF (Bhambri et al. 2011; Iturrizaga 2011).

Kedarnath is located at 3,533 m (30°44′05″N, 79°04′02″E), south of the confluence of the Mandakini and Saraswati rivers that originate from the Chorabari and Companion glaciers, respectively, about 1 and 0.7 km north of the village. Streamlets emanating from the surrounding ridges also contribute to these (Figs. 1, 2). The Chorabari and Companion glaciers shrunk considerably during the last few centuries and formed prominent lateral moraine ridges along their flanks (Chaujar 2009). Close to the present terminus of the Chorabari glacier, its right lateral moraine formed a barrier to a rain and snowmelt water fed stream that occupied a small deglaciated valley and created a 4.6-ha ephemeral lake known as the Chorabari *Tal* (3,845 m). The lake (or *Tal*) used to exist for a short period of time during and after the monsoon months (June–September). The water body had no visible outlet, and it probably used to drain by seeping through the porous moraines on its east and south (Fig. 3). The setting of the Chorabari lake, where lateral moraine of a trunk valley impounded the mouth of a tributary valley, is relatively less common but not unrecorded (Clague and Evans 2000; IAL 2009; Mool et al. 2011).

The major part of Kedarnath got devastated by a GLOF released from the Chorabari lake in the middle of June 2013. In this work, we attempted (1) to estimate various hydrological parameters including peak discharge of the GLOF event on the basis of available DEMs and predictive equations suggested by different authors, and (2) to compare between the pre- and post-event images of the area for assessing the damages caused to the Kedarnath village besides recording the geomorphic changes that occurred downstream of the lake.



Fig. 2 Physical setting of Kedarnath village in 2011. The retreat and shrinkage of the glaciers during the last ~ 130 years can be appreciated by comparing them with the facet marked 'X' in this photograph and in Fig. 4. A location of the Chorabari lake enclosed by the right lateral moraine of the Chorabari glacier; B Chorabari glacier; C Companion glacier; D Kedarnath settlement

2 Previous works

Glacial floods are fairly common in the Himalaya with a number of events reaching catastrophic dimensions (Richardson and Reynolds 2000). Reviews on the types and formation of glacial lakes and patterns of glacial floods were provided by Clague and Evans (2000), Richardson and Reynolds (2000), Iturrizaga (2011) and Westoby et al. (2014a). Glacial lakes of Uttarakhand were classified by Govindha Raj and Kumar (2013) using satellite images. Some recent studies on glacial floods in the Himalayan region include the works by Worni et al. (2013) in Kashmir, Himachal Pradesh and Uttarakhand; Govindha Raj (2010) in Zaskar; Ives (1986), Sakai et al. (2000), Quincey et al. (2007), Bolch et al. (2008), Bajracharya and Mool (2009), Mool et al. (2011), Lamsal et al. (2014) and Westoby et al. (2014b) in Nepal; Mool et al. (2001), Iwata et al. (2002), Fujita et al. (2008), Komori (2008) and Komori et al. (2012) in Bhutan; Yao et al. (2012) in Tibet; Govindha Raj et al. (2013) in Sikkim; and Ives et al. (2010) and Fujita et al. (2013) in different parts of Himalaya. Description of GLOF due to release of water from failure of lateral moraine, like the Kedarnath incident, is rare in the literature on Himalaya. At least one major event occurred in 1994 when a gap was opened in the left lateral moraine of the Luge glacier, Bhutan Himalaya (JAXA 2008; NASA-EO 2009).

The unprecedented Uttarakhand floods of June 2013 generated a large volume of scientific literature, and many of these referred to and/or described the events leading to the destructions at Kedarnath (Dubey et al. 2013; Rana et al. 2013; Sati 2013; Sati and Gahalaut 2013; Uniyal 2013; Kala 2014; Sharma and Kartikeyan 2014; Singh 2014). However, only three works specifically analysed the disaster per se. Dobhal et al. (2013)



Fig. 3 Chorabari lake in June 2011, viewing south. Note the portion of the moraine ridge that gave way to accumulating water on 17 June 2013

provided with the first technical explanation of the sequence of events at Kedarnath and its surroundings. Mishra and Srinivasan (2013) estimated rainfall patterns over Kedarnath from early June 2013 using meteorological satellite data. Durga Rao et al. (2014) attempted to simulate the floods in the Mandakini basin with reference to the Chorabari lake outburst on the basis of an elevation model from Cartosat data (CartoDEM) with 10-m posting. However, a few significant inconsistencies were noticed in this work (Bandyopadhyay and Kar 2014). In the present context, the chief of these includes wrong positioning of the Chorabari lake at the head of Kali Ganga, a left bank tributary to the Mandakini and consideration of only the flattish lake bed for the capacity estimation of the Chorabari, instead of up to the lowest elevation of the moraine ridge. The capacity of the Chorabari lake, estimated by Durga Rao et al. (2014), was $0.40 \times 10^6 \text{ m}^3$. This would have been much higher if the entire volume of the lake depression was considered, as done in the present study.

3 Background of the study

The antiquity of the Kedarnath settlement, developed around a famous Hindu temple with the same name, is not known for any certainty. Although the temple itself represents architectural style of early mediaeval period (Bali 2009), it probably was constructed sometime after the glaciers retreated following the LIA. A photograph taken by Carl L.

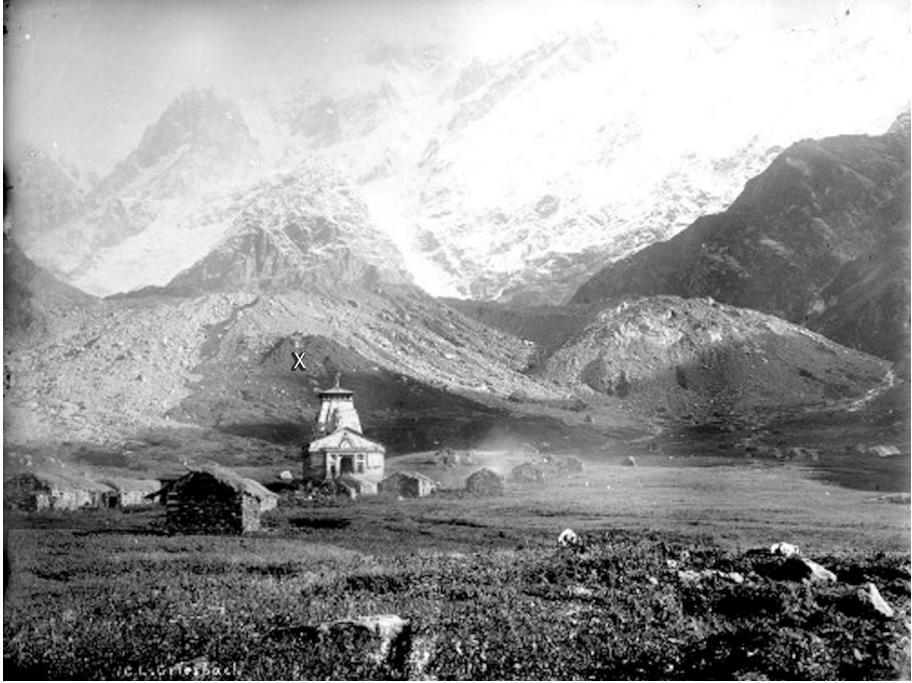


Fig. 4 Kedarnath temple area in 1882. Photograph taken by Carl L. Griesbach. See text for explanation (source: GSI 2013)

Griesbach in 1882 recorded ~ 10 hutments that lined the temple on a terrace of the Mandakini (Figs. 1d, 4). It also indicated that the masses of both Chorabari and Companion glaciers were markedly greater than the present, and their surface elevations were higher than the level of the lateral moraine ridges. Existence of the Chorabari lake at that time is unsure. The water body was not shown in Survey of India's topographical map 53N/NW (1:126,720), surveyed in 1923–1924. However, the subsequent edition of the map (53N/2, 1:50,000), surveyed in 1962, showed the lake prominently as did a 1965 Corona image (Fig. 5a). Some 83 years after Griesbach's photograph, the Corona image also indicated that Kedarnath village became well established in an elongated form and covered approximately 2.49 ha. By 2013, it expanded to 8.34 ha and became more congested (Figs. 2, 5b). The liner extension of the settlement was 520 m and had a southward gradient of 1:12.4, almost similar to the Mandakini, flowing on its west. Its elevation varied between 3,512 m in the south and 3,554 m in the north.

In June 2013, Kedarnath was reported to be affected by two separate events. First, a comparatively minor flash flood from the Saraswati catchment at 17:15 (India Standard Time) of 16 June, and second, a flood-cum-debris flow that occurred due to overflow and resulting outburst of the Chorabari lake at 06:45 on 17 June and draining of its water within 5–10 min (Dobhal et al. 2013). The later event caused unprecedented damage not only to Kedarnath but all along the Mandakini valley, many kilometres downstream (Rana et al. 2013; Singh 2014).

The high amount of rainfall that lead to the successive floods was termed 'unique' by the India Meteorological Department because it occurred due to a rare lower tropospheric convergence of a trough of westerlies, moisture-laden south-easterly monsoon winds and a

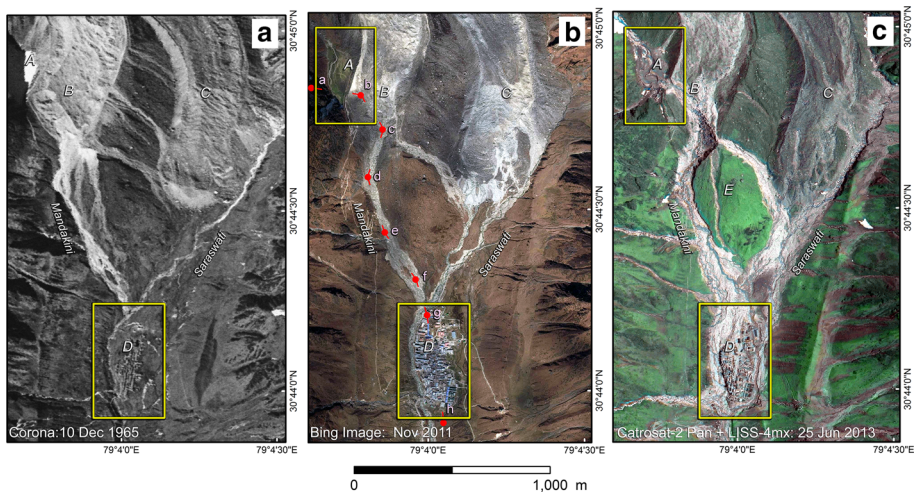


Fig. 5 Comparative images of the study area showing changes between 1965 and 2011 (46 years) and 2011 and 2013 (2 years). The areas marked in upper left and lower central portions of the images are enlarged as Figs. 7 and 9, respectively. *Line a–h* of Fig. 5b marks the elevation profile represented in Fig. 8 across the Chorabari lake and Kedarnath village along the shortest path taken by the GLOF. *A* Chorabari lake; *B* Chorabari glacier; *C* Companion glacier; *D* Kedarnath settlement; *E* Channel reactivated by the GLOF

north-moving low-pressure system that remained persistent over Uttarakhand for a long period (IMD 2013). The orographic effect of the Himalaya also aided the phenomenon (Dubey et al. 2013). A study by Mishra and Srinivasan (2013) used infrared and water vapour channels of *Meteosat-7* and indicated that the rainfall in a 5-km-square area around Kedarnath started picking up from 6 June 2013 and amounted to 347 mm up to 16 June 2014 (inclusive). Between 00:00 of 15 June and 07:00 of 17 June, hourly rainfall rates mostly stayed within 2–15 mm h⁻¹, touching or barely crossing 20 mm h⁻¹ on two occasions. Mishra and Srinivasan (2013) estimated that 84 mm of rain fell in the 24-h period up to 17:30 of 16 June 2013. Dobhal et al. (2013), on the other hand, reported that 325 mm of rainfall was recorded from the Chorabari glacier in the 24-h period preceding 17:00 of 16 June 2013 at an average rate of 17 mm h⁻¹. They also reported the presence of more than 2 m of snow cover in the catchment of the lake in early June. All these denote that the presence of antecedent moisture and incessant medium-intensity rains rather than cloudbursts was responsible for filling up of the Chorabari lake and that the rate of moisture input vastly exceeded loss by infiltration and evaporation. The discrepancy between the 24-h rainfall amounts stated by Mishra and Srinivasan (2013) and Dobhal et al. (2013) probably occurred because, while the former estimate was made indirectly from a 5-km² area around Kedarnath, the latter was gauged in situ, close to the Chorabari lake from which the GLOF originated. It may be noted here that no data are available on the rainfall that occurred specifically in the 12-h period after 17:00 of 16 June 2013 that lead to the breaching of the moraine dam and draining of the lake at 06:45 on the next day.

4 Materials and methods

We estimated the relief and other area parameters of the Chorabari lake and its outlet through the breached moraine ridge using three free-access digital elevation datasets from

Shuttle Radar Topography Mission (SRTM), Advanced Spaceborne Thermal Emission and Reflection Radiometer Global DEM (ASTER GDEM) and CartoDEM programmes (Table 1). Issues remain with most types of publicly available DEMs that are auto-generated on continental or global scale. SRTM, which is often used as a benchmark for ASTER and CartoDEM, itself incorporates an absolute height error of 6.2 m and a relative height error 8.7 m for 90 % of data in the Eurasia region (Rodríguez et al. 2006). Meyer et al. (2011) determined the vertical accuracy of ASTER GDEM (version 2), to be 8.68 m over United States and noted the existence of artefacts that can affect its utility in certain applications. Working in glacial lakes in Bhutan, Fujita et al. (2008) found that the root-mean-square errors of height differences of ground survey data from SRTM and purpose-generated ASTER DEMs were 11.3 and 11.0 m, respectively. The horizontal and vertical accuracy of CartoDEM, the coverage of which extends only over India, was reported to be 14 and 7 m, respectively, over hilly areas by Muralikrishnan et al. (2013). ISRO-NRSC (2011) stated that for the whole of India, vertical accuracy of 90 % of CartoDEM data with 90-m resolution was within 8 m of SRTM values. These error ranges pertain to absolute values while, to get reliable configuration of a small lake depression and its catchment, the accuracy of relative elevation is more important. One way of determining this is to see how well the DEM-generated topographical boundaries like lake and catchment perimeters agree with the maps or satellite images of the region. Field study of three lakes in Indian Himalaya by Worni et al. (2013) indicated that their topography was best depicted by SRTM data in two cases and ASTER GDEM in one case.

To compare the pre- and post-event scenarios of the area, we used three cloud-free high-resolution satellite images of 1965 (Corona, USGS), 2009 (Bing Maps) and 2013 (Cartosat-2 Pan + LISS-4mx, Bhuvan). We georeferenced and overlaid all these materials (Table 1) for the extraction of lake catchment area, height of moraine dam above the lakebed and bankful capacity of the lake (Table 2). Data on individual structures of Kedarnath destroyed due to the floods were also extracted.

Table 1 Elevation and image data used in the study

Data particulars	Imaging date	Average resolution (m)	Scene or tile identity	Data source
SRTM DEM	11 February 2000	85.1	SRTM3N30E079V1	earthexplorer.usgs.gov
ASTER GDEM version 2	2000–2009	28.7	ASTGDENV2_0N30E079	earthexplorer.usgs.gov
Cartosat-1 DEM (CartoDEM) version 1	2006–2008	28.6	H44H	bhuvan-noeda.nrsc.gov.in/download/download/download.php/
Corona KH4A-Aft image	10 December 1965	~4	DS1027-1007DA205_a	earthexplorer.usgs.gov
Bing image ^a	November 2011	~1	–	www.bing.com/maps imaging date from: http://mvexel.dev openstreetmap.org/bing/
Cartosat-1 Pan + LISS-4mx	25 June 2013	2.5	–	bhuvan3.nrsc.gov.in

^a Satellite information and exact date of pass of this image were not available

Table 2 Parameters of the Chorabari lake extracted from elevation data

Lake parameters	Cartosat-1 DEM (CD)	SRTM DEM (SD)	ASTER DEM (AD)	Average of CD & AD	Percentage difference between CD and AD	Percentage difference between SD and average of CD and AD
Absolute altitude of the lowest point on the moraine dam axis (m)	3,838	3,857	3,861	3,850	−0.6	−0.2
Maximum depth of water at full capacity (m)	11	12	15	13	−36.4	+8.3
Lake area at full capacity (m ²)	66,753	45,948	41,019	53,886	+38.6	+17.3
Volume of water at full capacity/storage capacity (10 ⁶ m ³)	0.62	0.43	0.25	0.43	+59.9	−0.2
Catchment area (ha)	271	291	267	269	+1.5	−7.6
Estimated rainfall required to fill the lake up to storage capacity excluding loss by evaporation and through flow (mm)	228	149	93	161	+59.2	+7.7

Quantification of debris flow following dam breach was attempted by many authors (Table 3); its major concerns include flow volume, peak discharge, breach width, breach height, failure time, front velocity of the flow, travel distance, and flow routing (Rickenmann 1999; Wahl 2004; Westoby et al. 2014a). In case of the Chorabari lake, volume of water and breach geometry was measured from the three DEMs used in the study (Table 2). Estimation of peak discharge (Q_p) was made by a number of predictive equations given by various authors (Table 3). The parameters taken were storage (S), height of water (H), breach width (B) and gravity (g). The equations were grouped into four categories where peak discharge was considered as function (f) of various parameters

$$Q_p = f(H)$$

$$Q_p = f(S)$$

$$Q_p = f(H, S)$$

$$Q_p = f(H, B, g)$$

5 Results and discussion

5.1 Lake parameters and discharge estimations

It was assumed, as per Dobhal et al. (2013), that the breaching of the Chorabari lake on 17 June 2013 was initiated by overtopping of the accumulated rainwater over the lateral moraine ridge (Figs. 3, 6). The lowest absolute height of the ridge on the south-east of the lake was determined as 3,838 m, 3,857 m and 3,861 m by CartoDEM (CD), SRTM DEM (SD) and ASTER GDEM (AD), respectively. In all three DEMs, this point closely

Table 3 GLOF peak discharge and lake volume derived from SRTM elevation data and predictive equations

Equations	Peak discharge (cumec)	Computed storage volume from peak discharge ^a (10^6 m^3)	Percentage difference in computed storage volume from DEM-derived storage volume ^b
<i>Category-1: peak discharge as a function of height of water</i>			
Kirkpatrick (1977): $Q_p = 1.268(H + 0.3)^{2.5}$	432	0.001	+29.8
US Soil Conservation (1981): $Q_p = 16.6(H)^{1.85}$	1,175	0.35	-18.9
US Bureau of Reclamations (1982): $Q_p = 19.1(H)^{1.85}$	1,352	0.40	-6.7
Singh and Snorrason (1982): $Q_p = 13.4(H)^{1.89}$	1,040	0.31	-28.2
Walder and O'Connor (1997): $Q_p = 60.3(H)^{0.84}$	417	0.12	-71.2
Pierce et al. (2010): $Q_p = 0.784(H)^{2.688}$	382	0.11	-73.6
<i>Category-2: peak discharge as a function of storage</i>			
Singh and Snorrason (1984): $Q_p = 1.776(S)^{0.47}$	793	0.24	-45.3
Evans (1986): $Q_p = 0.72(S)^{0.53}$	700	0.21	-51.7
Walder and O'Connor (1997): $Q_p = 0.045(S)^{0.66}$	237	0.07	-83.7
Costa (1985): $Q_p = 1.22(S)^{0.57}$	1,994	0.60	+37.6
<i>Category-3: peak discharge as a function of height of water and storage</i>			
Hagen (1982): $Q_p = 0.54(SH)^{0.5}$	1,125	0.34	-22.3
McDonald and Langridge-Monopolis (1984): $Q_p = 1.154(SH)^{0.412}$	626	0.19	-56.8
McDonald and Langridge-Monopolis (1984): $Q_p = 3.85(SH)^{0.411}$	2,058	0.62	+42.0
Costa (1985): $Q_p = 0.981(SH)^{0.42}$	602	0.18	-58.5
Costa (1985): $Q_p = 2.634(SH)^{0.44}$	2,194	0.66	+51.4
Froehlich (1995): $Q_p = 0.607(S^{0.295}H^{1.24})$	486	0.15	-66.5
Walder and O'Connor (1997): $Q_p = 0.19(SH)^{0.47}$	250	0.07	-82.7
Pierce et al. (2010): $Q_p = 0.0176(SH)^{0.606}$	185	0.06	-87.2
Pierce et al. (2010): $Q_p = 0.038(S^{0.475}H^{1.09})$	223	0.07	-84.6
<i>Category-4: peak discharge as a function of breach cross sectional area and gravity</i>			
Hungr et al. (1984): $Q_p = 0.3 B g^{0.5} H^{1.5}$	1,783	0.53	+23.0

Q_p , peak discharge; S , storage; H , height of water; B , breach width; g gravitational acceleration

^a Based on the assumption that the lake completely drained in 10 min and that the discharge diminished linearly from the peak (see text for further explanation)

^b Values closest to zero indicate closest match of the storage volume computed from peak discharge with storage volume estimated from SRTM DEM ($0.43 \times 10^6 \text{ m}^3$)

coincided with the location of breaching indicated by the merged Catrosat-1 Pan + LISS-4mx image of 25 June 2013 (Figs. 3, 7). Its actual height, however, is likely to be somewhat different from the above elevations because the 28-m (CD and AD) or 85-m (SD) DEM pixels represented average altitudinal values (Fig. 6). The lowest relative height

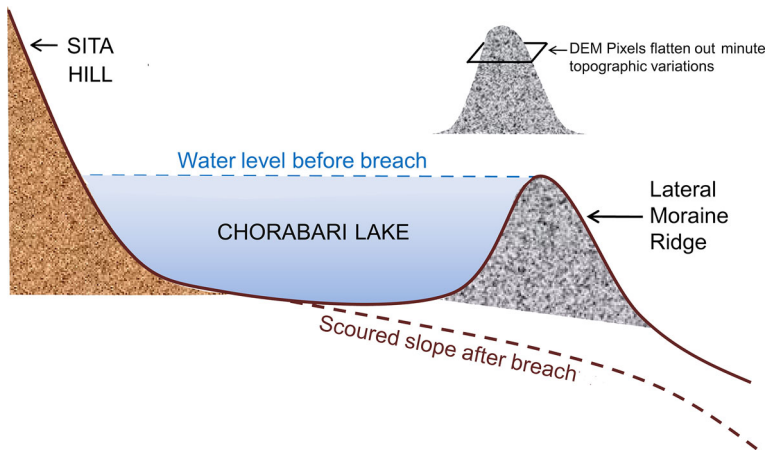


Fig. 6 Schematic pre- and post-GLOF profiles across the Chorabari lake, from west to east through the point of outburst (not to scale). The volume of floodwater estimated in the study is based on the lowest elevation of the DEM pixel situated on the central axis of the moraine ridge that coincided with the breached portion shown in Figs. 3 and 7b. The elevation is likely to be somewhat different from actual because every DEM pixel averages out all topographical variations within its perimeter

of the ridge from the lake bed amounted to 11 m (CD), 12 m (SD) and 15 m (AD). Based on these values, contours were generated to indicate the bankful capacity of the lake prior to its breaching (Fig. 7), which amounted to $0.63 \times 10^6 \text{ m}^3$ (CD), $0.43 \times 10^6 \text{ m}^3$ (SD) and $0.25 \times 10^6 \text{ m}^3$ (AD).

With lack of field data, the accuracy of the DEMs had to be determined indirectly. In most cases, the CD- and AD-derived figures represented two extremes of the three datasets with crucial lake parameters like depth, area and volume of water at storage capacity varying between 36 and 60 %. The SD, on the other hand, represented the values that are very close to the average of CD and SD figures with variations ranging between 0.2 and 17 % (Table 2). More significantly, the lake boundary as well as the lake watershed derived from SAR-based SRTM data fitted much better to the topography represented in the satellite images than the other two optical elevation datasets (Fig. 7a). The SRTM-derived information, therefore, was employed for further discharge-related analyses in this study despite its coarser resolution.

Using the SRTM-derived information, it was estimated that it would require 149 mm of rainfall in its 791-ha catchment area to fill the Chorabari lake up to its capacity, without considering loss from seepage or evaporation. Gain from antecedent water already present in the lake and snow from the last season reported to be present in the area (Dobhal et al. 2013) was also not taken into account due to the unavailability of data. The estimate was only 45 % of 325 mm—the rainfall figure provided by Dobhal et al. (2013) for 24-h period up to 17:00 of 16 June 2013—connoting huge loss from seepage through the pervious morainic materials. This also confirmed that more than enough rainfall occurred in the area for filling the lake up to its storage capacity.

Haeberli (1983) noted that in the case of glacial dam burst, peak discharge coincides with the frontal wave following the breach. Following this principle, it was assumed that the initial discharge subsequent to the breach is the highest (peak discharge, Q_p). Reliability of the estimated results derived from the equations was assessed by comparing them

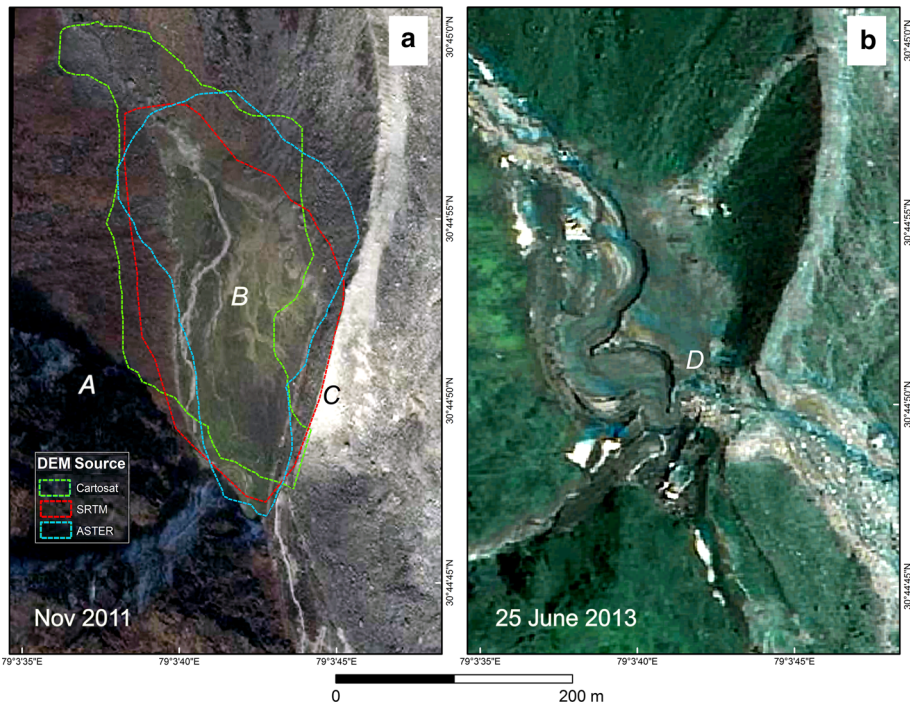


Fig. 7 Pre- and post-GLOF images of the Chorabari lake region. Extents of the lake at full capacity are shown in **a** as extracted from the three DEMs. The perimeter derived from the SRTM DEM matches with the topography most suitably. **A** Sita hill; **B** Flattish lake bed in the dry post-monsoon season; **C** Right lateral moraine of the Chorabari glacier; **D** Breached portion of the moraine ridge with incised channels that scoured the lacustrine deposits during draining of the lake

with the observation that after reaching the peak discharge at source, the lake emptied in the next 10 min, which is the outer limit of draining time mentioned by Dobhal et al. (2013). A linear drop in lake water and discharge rate was presumed. By integrating a linearly diminishing discharge rate during a 10-min period, the total volume of water discharged from the lake was measured for each equation. Next, by comparing the volume of discharge derived for the 10-min period with the volume of lake water estimated from the SRTM dataset (Table 2), most appropriate predictive equation was found to be the one given by the United States Bureau of Reclamations (1982) of the first category. This came to within 6.7 % of the SRTM-derived value (Table 3). The equation predicted 1,352 cumecs of peak discharge from the lake.

5.2 Downstream changes

Inspection of the 2011 image of the glacial outwash features above Kedarnath denoted that apart from taking the usual southward route from the snout of the Chorabari glacier, the meltwater also used to issue towards the south-east through a fairly steep gully in the direction of the Saraswati. In 1965, at least five gullies were well established on the left lateral moraine of the Chorabari glacier (Fig. 5a), out of which only this one remained active 48 years later (Fig. 5b). The number of south-flowing streamlets issuing from the

snout region also dwindled from three to one. This probably connoted either a reduction in precipitation amount and/or a drop in water discharge from the glacier since 1965. A comparison between the 2011 and 2013 images showed that a new gully was opened on the east of and sub-parallel to the main south-flowing channel to accommodate the GLOF-generated debris flow (marked 'E' in Fig. 5c). This, however, was a reactivation of one of the old disused 1965 streamlets mentioned earlier. It can also be inferred from the scarps established in the streambeds by the 2013 debris flow that the bulk of the water and slope materials that devastated Kedarnath followed the more direct southward channel rather than the eastward gully towards the Saraswati. As the debris started to fan out at the break of slope below 3,650 m (point 'e' in Figs. 5b, 8), the width of lower portions of both the channels increased by more than four times.

Kedarnath was situated 300 m lower than the bed level of the Chorabari lake. From the breached portion of the moraine ridge, the debris flow triggered by the GLOF mostly followed 1.41 km of existing channels to reach the northern end of the village. As it went down, it entrained morainic materials as well as lacustrine sediments from the bed of the lake itself (Figs. 6, 7b). As shown by the pre-event images of Figs. 2, 5b and 9b, but not clearly represented in the elevation profiles apart from the one derived from CartoDEM (Fig. 8), the bed level of the Mandakini was lower than the terrace at the northern end of the village where the river joined the Saraswati and slightly recurved towards the west (Figs. 1, 2). The presence of channel training structures along the left bank of the Mandakini in this region (Fig. 9b) indicates that threat from ingress of floodwaters into the settlement already existed. The debris flow of 17 June 2013 could easily overcome the altitudinal difference between the river bed and the terrace and overwhelmed the village. The comparatively minor flash flood of the Saraswati on the previous day might had aided in filling up of the river channel and provided the GLOF debris with a more direct access into Kedarnath.

The elevation profiles along downstream path of the GLOF showed noticeably better consistency between AD and SD than between CD and the other two (Fig. 8). The average deviations of the AD-generated and CD-generated profiles were +9.9 and -13.2 m from the SD-derived profile, respectively. The ranges of deviations were +26.94 to +0.81 m (27.8 m) and -43.59 to +22.27 m (66.2 m) in that order.

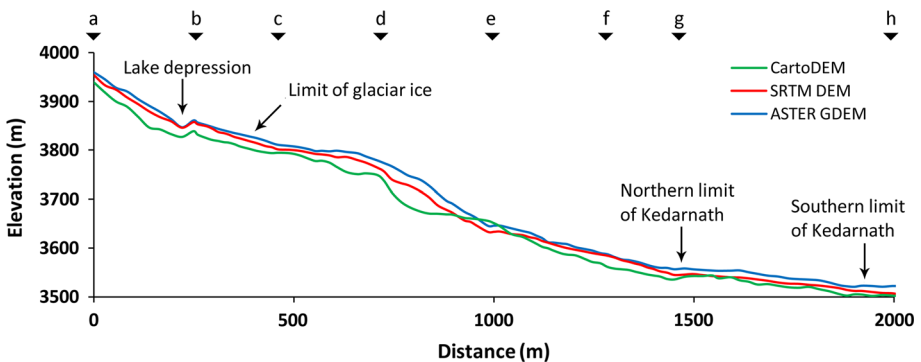


Fig. 8 Topographical profiles along the shortest path taken by the GLOF from the Chorabari lake through the village of Kedarnath (marked a–h in Fig. 5b). Vertical exaggeration: 1.2×

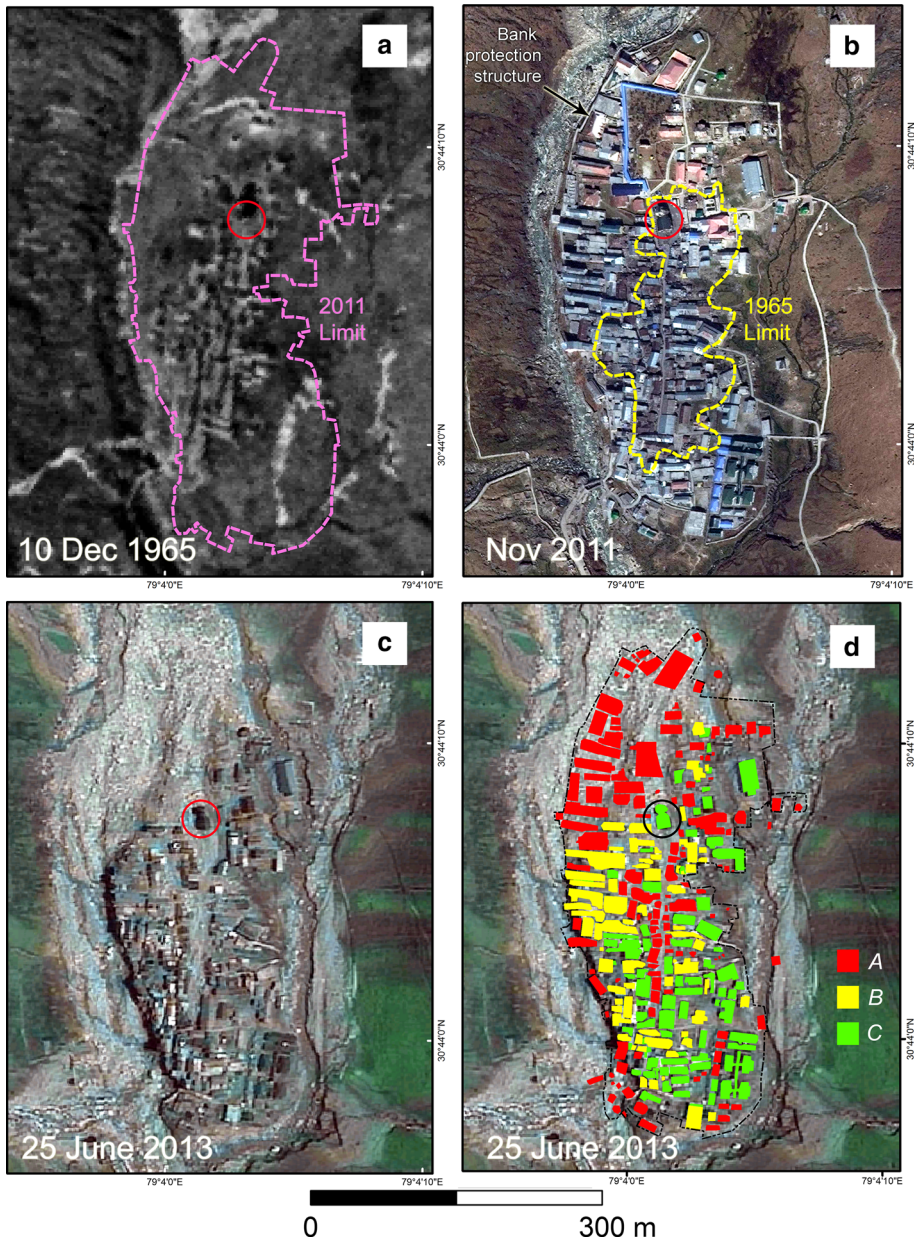


Fig. 9 Pre- and post-GLOF images of Kedarnath village. The area of the settlement, indicated by *dashed lines* in **a, b**, increased more than three times between 1965 and 2011. The flood event of 2013 completely destroyed 53 % of its structures and partly damaged another 22 % (**c, d**). *A* Completely destroyed structures; *B* Partly destroyed structures; *C* Slightly affected or unaffected structures. *Circles* denote the location of Kedarnath temple that emerged mostly unharmed after the floods

Table 4 Pre- and post-event status of individual structures of Kedarnath settlement

Post-event condition of structures	Number	Pre-event roof area (m ²)	Post-event roof area (m ²)
Completely wiped out	138	16,491.0	0.0
Partly destroyed	56	9,962.6	7,287.2
Slightly affected or unaffected	65	10,845.4	10,845.4
Total	259	37,299.0	18,132.6

The downstream consequences of the debris flow were evident from the comparison of pre- and post-event images of Kedarnath village (Fig. 9d). The north-western section of the hamlet was on the direct path of the debris flow and took most of the brunt. Almost all structures of this area were destroyed or buried without trace. With a gradient of 1:12.4, the path running through the centre of the settlement acted as a major conduit of the flow and strings of destroyed buildings lined its periphery (Fig. 9c, d). Most of the partially destroyed or partly damaged structures occupied the area adjacent to and downslope of the razed portion of the settlement. The southern and south-eastern sections of the village were least affected. Out of 37,299 m² of pre-event roof area of Kedarnath (259 structures), 44.2 % were completely destroyed and 26.7 % were partly damaged, representing 138 and 56 structures, respectively. In the partly destroyed structures, 26.9 % of roof area was gone. Only one-fourth of the structures of the village emerged intact or slightly affected after the event (Table 4). One notable structure that emerged unharmed was the Kedarnath temple. Made of massive slabs of granites and gneisses (Bali 2009; Chaujar 2009), it was able to withstand the onslaught of the debris-laden floodwater despite its location in the northern part of the settlement.

6 Conclusions

Occurrence of GLOF from a lateral moraine-dammed lake is rare. It occurred in Chorabari mainly because of the collapsed barrier's proximal location to the snout of the glacier that directly overlooked the Mandakini valley and the village of Kedarnath, some 300 m below. The study confirmed that more than adequate rainfall occurred in its 291-ha catchment to fill up the Chorabari lake to its 0.43×10^6 m³ capacity prior to the occurrence of the GLOF that attained a peak discharge of 1,352 cumecs. Post-event satellite image indicated that bulk of the debris flow travelled through the main channel of the Mandakini river and entered the village from the north-west. The pattern of damages to the homesteads and other structures in Kedarnath also agreed to this. The study also demonstrated the problems associated with measuring the volume of small depressions using DEM data available in the Internet as the results tend to vary extensively. Employing this kind of data in the prediction of GLOF needs to be done with appropriate caution.

Acknowledgments We thank Dr. Amal Kar for his advice and help in formulation of this article. Mr. Ratanlal Biswas kindly allowed us to use two photographs from his collection. We also thank the agencies from which the elevation and satellite data were sourced: United States Geological Survey (Corona, SRTM DEM and ASTER GDEM), India's National Remote Sensing Centre (CartoDEM and post-event image), and Bing Map (pre-event image).

References

- Bajracharya SR, Mool P (2009) Glaciers, glacial lakes and glacial lake outburst floods in the Mount Everest region, Nepal. *Ann Glaciol* 50(53):81–86
- Bali R (2009) Advance and retreat of Chaurabari glacier. *Curr Sci* 97:471
- Bandyopadhyay S, Kar NS (2014) The Kedarnath disaster: in search of scientific reasoning. *Curr Sci* 107:557
- Bhambri R, Bolch T, Chaujar RK, Kulshreshtha SC (2011) Glacier changes in the Garhwal Himalaya, India, from 1968 to 2006 based on remote sensing. *J Glaciol* 57:543–556
- Bolch T, Buchroithner MF, Peters J, Baessler M, Bajracharya S (2008) Identification of glacier motion and potentially dangerous glacial lakes in the Mt. Everest region/Nepal using spaceborne imagery. *Nat Hazards Earth Syst Sci* 8:1329–1340
- Chaujar RK (2009) Climate change and its impact on the Himalayan glaciers: a case study on the Chorabari glacier, Garhwal Himalaya, India. *Curr Sci* 96:703–708
- Clague JJ, Evans SG (2000) A review of catastrophic drainage of moraine-dammed lakes in British Columbia. *Quat Sci Rev* 19:1763–1783
- Costa JE (1985) Floods from dam failures. US Geological Survey, Open-File Rep. No. 85-560. <http://pubs.usgs.gov/of/1985/0560/report.pdf>. Accessed 24 April 2014
- Dobhal DP, Gupta AK, Mehta M, Khandelwal DD (2013) Kedarnath disaster: facts and plausible causes. *Curr Sci* 105:171–174
- Dubey SC, Shukla DP, Ningreihon AS, Usham AL (2013) Orographic control of the Kedarnath disaster. *Curr Sci* 105:1474–1476
- Durga Rao KHV, Rao VV, Dadhwal VK, Diwakar PG (2014) Kedarnath flash flood: a hydrological and hydraulic simulation study. *Curr Sci* 106:598–603
- Evans SF (1986) The maximum discharge of outburst floods caused by the breaching of man-made and natural dams. *Can Geotech J* 23:385–387
- Froehlich DC (1995) Peak outflow from breached embankment dam. *J Water Resour Plan Manag* 121:90–97
- Fujita K, Suzuki R, Nuimura T, Akiko S (2008) Performance of ASTER and SRTM DEMs, and their potential for assessing glacial lakes in the Lunana region, Bhutan Himalay. *J Glaciol* 54:220–228
- Fujita K, Sakai A, Takenaka S, Nuimura T, Surazakov AB, Sawagaki T, Yamanakuchi T (2013) Potential flood volume of Himalayan glacial lakes. *Nat Hazards Earth Syst Sci* 13:1827–1839
- Govindha Raj KB (2010) Remote sensing based hazard assessment of glacial lakes: a case study from Zanskar basin, Jammu and Kashmir. *Geomat Nat Hazards Risk* 1:339–347
- Govindha Raj KB, Kumar V (2013) Glacial lakes in Uttarakhand: a remote sensing perspective. National Remote Sensing Centre, Indian Space Research Organisation, Hyderabad. <http://www.nrsc.gov.in/pdf/uk.pdf>. Accessed 20 April 2014
- Govindha Raj KB, Remya SN, Kumar KV (2013) Remote sensing-based hazard assessment of glacial lakes in Sikkim Himalaya. *Curr Sci* 104:359–364
- GSI: Geological Survey of India (2013) Photo Archive: Carl Griesbach in Hundes and Spiti—Section II. http://www.portal.gsi.gov.in/portal/page?_pageid=127,763858&_dad=portal&_schema=PORTAL. Accessed 25 Nov 2013
- Haerberli W (1983) Frequency and characteristics of glacier floods in the Swiss Alps. *Ann Glaciol* 4:85–90
- Hagen VK (1982) Re-evaluation of design floods and dam safety. In: Proceedings of the 14th congress of international commission on large dams. International Commission on Large Dams, Paris
- Hungr O, Morgan GC, Kellerhals R (1984) Quantitative analysis of debris torrent hazards for design of remedial measures. *Can Geotech J* 21:663–677
- IAL: International Association of Limnogeology (2009) Lake origins. <http://www.ohio.edu/Geology/ial/limnogeology/LakeOrigins.html> Accessed 30 Nov 2014
- IMD: India Meteorological Department (2013) A preliminary report on heavy rainfall over Uttarakhand during 16–18 June 2013 http://www.wimd.gov.in/doc/uttarakhand_report_04_09_2013.pdf. Accessed 20 April 2014
- ISRO-NRSC: Indian Space Research Organisation—National Remote Sensing Center (2011) Evaluation of Indian national DEM from Cartosat-1 data: summary report ver 1. http://bhuvan-noeda.nrsc.gov.in/download/download/tools/document/CaroDEMReadme_v1_u1_23082011.pdf. Accessed 10 June 2014
- Iturrizaga L (2011) Glacier lake outburst floods. In: Singh VP, Singh P, Haritashya UK (eds) Encyclopedia of snow, ice and glaciers. Springer Science, Dordrecht, pp 381–399
- Ives JD (1986) Glacial lake outburst floods and risk engineering in the Himalaya. International Centre for Integrated Mountain Development, Occasional Paper 5:1–41

- Ives JD, Shrestha RB, Mool PK (2010) Formation of glacial lakes in the Hindu Kush-Himalayas and GLOF risk assessment. International Centre for Integrated Mountain Development, Kathmandu
- Iwata S, Ageta Y, Naito N, Sakai A, Narama C, Karma (2002) Glacial lakes and their outburst flood assessment in the Bhutan Himalaya. *Global Environ Res* 6:3–17
- JAXA: Japan Aerospace Exploration Agency (2008) Glacial lakes in Bhutan Himalayas. <http://www.eorc.jaxa.jp/en/imgdata/topics/2008/tp080402.html>. Accessed 15 Nov 2014
- Kala CP (2014) Deluge, disaster and development in Uttarakhand Himalayan region of India: challenges and lessons for disaster management. *Int J Disaster Risk Reduct* 8:143–152
- Kirkpatrick, GW (1977) Evaluation guidelines for spillway adequacy in the evaluation of dam safety. In: Proceedings engineering foundation conference, Pacific Grove, California, American Society of Civil Engineers, pp 395–414
- Komori J (2008) Recent expansions of glacial lakes in the Bhutan Himalayas. *Quat Int* 184:177–186
- Komori J, Koike T, Yamanokuchi T, Tshering P (2012) Glacial lake outburst events in the Bhutan Himalayas. *Global Environ Res* 16:59–70
- Lamsal D, Sawagaki T, Watanabe T, Byers AC (2014) Assessment of glacial lake development and prospects of outburst susceptibility: Chamlang South glacier, eastern Nepal Himalaya. *Geomat Nat Hazards Risk*. doi:10.1080/19475705.2014.931306
- Mcdonald TC, Langridge-Monopolis J (1984) Breaching characteristics of dam failures. *J Hydraul Eng* 110:567–586
- Meyer D et al. (2011) ASTER global digital elevation model version 2: summary of validation results. http://www.jspacesystems.or.jp/ersdac/GDEM/ver2Validation/Summary_GDEM2_validation_report_final.pdf. Accessed 10 June 2014
- Mishra A, Srinivasan J (2013) Did a cloud burst occur in Kedarnath during 16 and 17 June 2013? *Curr Sci* 105:1351–1352
- Mool PK, Wangda D, Bajracharya SR, Kunzang K, Gurung DR, Joshi SP (2001) Inventory of glaciers, glacial lakes and glacial lake outburst floods, monitoring and early warning systems in the Hindu Kush-Himalaya region: Bhutan. International Centre for Integrated Mountain Development, Kathmandu
- Mool PK, Maskey PR, Koirala A, Joshi SP, Lizong W, Shrestha AM, Eriksson M, Gurung B, Pokharel B, Khanal NR, Panthi S, Adhikari T, Kayastha RB, Ghimire P, Thapa R, Shrestha B, Shrestha S (2011) Glacial lakes and glacial lake outburst floods in Nepal. International Centre for Integrated Mountain Development, Kathmandu
- Muralikrishnan D, Pillai A, Narender B, Reddy S, Venkataraman VR, Dadhwal VK, Raghu V (2013) Validation of Indian National DEM from Cartosat-1 Data. *J Ind Soc Remote Sens* 41:1–13
- NASA-EO: National Aeronautics and Space Administration—Earth Observatory (2009) Thorthormi glacier lake, Bhutan. <http://earthobservatory.nasa.gov/IOTD/view.php?id=40962>. Accessed 15 Nov 2014
- Pierce MW, Thornton CI, Abt SR (2010) Predicting peak outflow from breached embankment dams. *J Hydrol Eng* 15:338–349
- Quincey DJ, Richardson SD, Luckman A, Lucas RM, Reynolds JM, Hambrey MJ, Glasser NF (2007) Early recognition of glacial lake hazards in the Himalaya using remote sensing datasets. *Glob Planet Chang* 56:137–152
- Rana N, Singh S, Sundriyal YP, Juyal N (2013) Recent and past floods in Alakananda valley: causes and consequences. *Curr Sci* 105:1209–1212
- Richardson SD, Reynolds JM (2000) An overview of glacial hazards in the Himalayas. *Quat Int* 65(66):31–47
- Rickenmann D (1999) Empirical relationship for debris flows. *Nat Hazards* 19:47–77
- Rodríguez E, Morris CS, Belz JE (2006) A global assessment of the SRTM performance. *Photogramm Eng Remote Sens* 72:249–260
- Sakai A, Chikita K, Yamada T (2000) Expansion of a moraine-dammed glacial lake, Tsho Rolpa, in Rolwaling Himal, Nepal Himalaya. *Limnol Oceanogr* 45:1401–1408
- Sati VP (2013) Extreme weather related disaster, a case study of two flash flood hit areas of Badrinath and Kedarnath Valleys, Uttarakhand Himalaya, India. *J Earth Sci Eng* 3:562–568
- Sati SP, Gahalaut VK (2013) The fury of floods in north-west Himalayan region: the Kedarnath tragedy. *Geomat Nat Hazards Risk* 4:193–201
- Sharma A, Kartikeyan D (2014) Potential of CartoDEM in disaster management. *J Geomat* 8:96–100
- Sharma MC, Owen LA (1996) Quaternary glacial history of NW Garhwal, central Himalayas. *Quat Sci Rev* 15:335–365
- Singh DS (2014) Surface processes during flash floods in the glaciated terrain of Kedarnath, Garhwal Himalaya and their role in the modification of landmass. *Curr Sci* 106:594–597

- Singh KP, Snorrason A (1982) Sensitivity of outflow peaks and flood stages to the selection of dam breach parameters and simulation models, vol 288. SWS Contract Report, Illinois Department of Energy and Natural Resources, State Water Survey Division, University of Illinois
- Singh KP, Snorrason A (1984) Sensitivity of outflow peaks and flood stages to the selection of dam breach parameters and simulation models. *J Hydrol* 68:295–310
- United States Bureau of Reclamation (1982) Guidelines for defining inundated areas downstream from Bureau of Reclamation dams. US Department of the Interior, Bureau of Reclamation, Denver
- United States Soil Conservation Service (1981) Simplified dam-breach routing procedure. Technical Release 66
- Uniyal A (2013) Lessons from Kedarnath tragedy of Uttarakhand Himalaya, India. *Curr Sci* 105:1472–1474
- Wahl TL (2004) Uncertainty of predictions of embankment dam breach parameters. *J Hydraul Eng* 5:389–397
- Walder JS, O'Connor JE (1997) Methods for predicting peak discharge of floods caused by failure of natural and constructed earthen dams. *Water Resour Res* 33:2337–2348
- Westoby MJ, Glasser NF, Brasington J, Hambrey MJ, Quincey DJ, Reynolds JM (2014a) Modelling outburst floods from moraine-dammed glacial lakes. *Earth Sci Rev* 134:137–159
- Westoby MJ, Glasser NF, Hambrey MJ, Reynolds JM, Hassan AAM (2014b) Reconstructing historic glacial lake outburst floods through numerical modelling and geomorphological assessment: extreme events in the Himalaya. *Earth Surf Process Landf*. doi:10.1002/esp.3617
- Worni R, Huggel C, Stoffel M (2013) Glacial lakes in the Indian Himalayas: from an area-wide glacial lake inventory to on-site and modeling based risk assessment of critical glacial lakes. *Sci of the Total Environ* 468–469(Supplement 1):S71–S84
- Yao X, Liu S, Sun M, Wei J, Guo W (2012) Volume calculation and analysis of the changes in moraine-dammed lakes in the north Himalaya: a case study of Longbasaba lake. *J Glaciol* 58:753–800